Jurnal Geografi Gea
Journal homepage: https://ejournal.upi.edu/index.php/gea

# Machine Learning for Paddy Mapping Based on Agroecological Data and Multispectral Imagery

*Riki Ridwana [1,3], Muhammad Kamal [2*], Sanjiwana Arjasakusuma[2]*

*[1]Doctoral Program in Geographical Science, Faculty of Geography, Universitas Gadjah Mada, Sekip Utara, Bulaksumur, 55281, Yogyakarta, Indonesia*
*[2]Department of Geographic Information Science, Faculty of Geography, Universitas Gadjah Mada, Sekip Utara, Bulaksumur, 55281, Yogyakarta, Indonesia*
*[3]Mapping Survey and Geographic Information Study Program, Faculty of Social Sciences Education, Universitas Pendidikan Indonesia, Jalan Doktor Setiabudi No 229, 40154, Bandung, Indonesia.*

*Correspondence e-mail: m.kamal@ugm.ac.id

**ABSTRACT**

Accurate and up-to-date spatial information on paddy cultivation is essential for ensuring national food security, particularly in agrarian countries such as Indonesia. However, conventional mapping approaches often fail to capture spatial heterogeneity driven by diverse agroecological conditions. This study develops a machine learning–based paddy mapping framework by integrating multispectral Sentinel-2 imagery with agroecological variables to improve classification accuracy and model transferability. The analysis incorporates spectral features and vegetation indices derived from Sentinel-2 data, along with environmental variables such as rainfall, elevation, slope, and landform characteristics. Support Vector Machine (SVM) and Random Forest (RF) classifiers were trained and validated using reference data obtained from field surveys and official government records. Model performance was evaluated using confusion matrices, overall accuracy, F1-score, and the Kappa coefficient. Results show that both RF and SVM achieved overall accuracies exceeding 90% when agroecological variables were included, with RF consistently outperforming SVM across all evaluation metrics. The integration of agroecological data significantly improved classification reliability compared to spectral-only approaches, particularly in heterogeneous tropical landscapes. The proposed framework demonstrates strong potential for scalable, transferable agricultural mapping, supporting precision farming, irrigation planning, and sustainable food security management.

© 2026, FPIPS UPI. Open access article under the CC BY-SA license

**ARTICLE INFO**

***Article History:***
*Submitted/Received 03 September 2025*
*First Revised 25 January 2026*
*Accepted 21 April 2026*
*First Available online 29 April 2026*
*Publication Date 30 April 2026*

***Keywords:***
*Machine learning,*
*Paddy mapping,*
*Agroecological,*
*Multispectral imagery*

## 1. INTRODUCTION

Agriculture is a strategic sector that plays a crucial role in ensuring food security, particularly in agrarian countries such as Indonesia, where rice is the primary staple food for the majority of the population (Khanal et al., 2020; Klerkx et al., 2019; Singh et al., 2022). One of the main commodities in the national food system is paddy, which becomes the main material of consumption for the majority of residents (Kadir et al., 2019). Paddy cultivation dominates agricultural landscapes and directly influences national food resilience and socio-economic stability. Therefore, the availability of accurate, up-to-date, and spatially explicit information on paddy distribution and extent is essential to support evidence-based agricultural planning and policy formulation. However, conventional paddy inventory methods rely heavily on field surveys, which are time-consuming, costly, spatially limited, and often unable to provide timely information at regional to national scales (Prasetya and Danoedoro, 2019; Ridwana et al., 2025; Putra et al., 2018).

Advances in remote sensing (RS) technology have provided an effective solution for large-scale agricultural monitoring due to their synoptic coverage, high temporal frequency, and consistent data acquisition (Arrafi et al., 2022; Stevens, 2015; Tun, 2022; Zhao et al., 2021). Multispectral satellite imagery, particularly from the Sentinel-2 mission, has been widely used for paddy mapping owing to its fine spatial resolution (10–20 m), high revisit frequency (5 days), and the availability of red-edge and near-infrared bands that are highly sensitive to vegetation phenology and crop growth stages (Dharma et al., 2022; Song et al., 2021; Veloso, 2017). Paddy fields exhibit distinctive temporal spectral characteristics during flooding, transplanting, vegetative growth, and harvesting phases, which multispectral observations can effectively capture. Consequently, multispectral imagery has proven to be highly suitable for distinguishing paddy fields from other land cover types in tropical agricultural environments (Nguyen, 2020; Ni et al., 2021; Yang et al., 2022). However, the main challenge in using satellite images for paddy mapping is the variation in agroecological conditions across regions, which affects plant spectral response and reduces mapping accuracy if the classification model does not account for local characteristics.

Paddy mapping using spectral information alone remains challenging, particularly in regions with complex agroecological conditions. Variations in topography, irrigation systems (irrigated and rainfed), rainfall regimes, and landforms can significantly influence planting calendars, crop growth dynamics, and spectral responses of paddy fields (Gumma et al., 2022; Murti, 2017). In Indonesia, paddy is cultivated across diverse agroecological zones, ranging from lowland irrigated plains to rainfed upland areas with varying slopes, elevations, and microclimates. These heterogeneities often reduce classification accuracy when local environmental characteristics are not explicitly incorporated into mapping models (Gaznayee, 2019; Lee et al., 2020).

Machine learning (ML) approaches have demonstrated strong potential to improve paddy mapping accuracy by capturing complex, non-linear relationships between spectral features and environmental variables (Ridwana et al., 2022; W. Zhang et al., 2020). Algorithms such as Random Forest (RF), Support Vector Machine (SVM), and Deep Neural Network (DNN) have been extensively applied in agricultural remote sensing due to their robustness to noise, ability to handle high-dimensional data, and superior classification performance compared to conventional statistical methods (Ridwana et al., 2024, 2025; L. Wang, Wang, Liu, et al., 2022). Image data merging multispectral with variables, such as agroecological factors like rainfall, elevation, slope, direction, face slopes, and landforms, can significantly increase model performance (Gaznayee, 2019; Lee et al., 2020; Murti, 2017). In particular, RF and SVM have

DOI: https://doi.org/10.17509/gea.v26i1.89942
p-ISSN 1412-0313 e-ISSN 2549-7529

been widely reported as effective and stable classifiers for paddy mapping using multispectral imagery, especially in heterogeneous agricultural landscapes (Dang et al., 2021; Noi, 2018; Teluguntla et al., 2018; Yang and Li, 2022).

Recent studies indicate that integrating multispectral imagery with agroecological variables—such as rainfall, elevation, slope, aspect, landform, and hydrological conditions—can significantly enhance paddy classification accuracy by providing contextual information related to crop suitability and growth conditions (Gaznayee, 2019; Lee et al., 2020; Murti, 2017). Agroecological information is particularly important for paddy mapping because rice cultivation is highly dependent on water availability, terrain characteristics, and climate variability, which directly influence cropping patterns and phenological responses. Despite these advances, systematic integration of agroecological data with machine learning-based paddy mapping remains limited in Indonesia, especially studies that explicitly evaluate the contribution of agroecological variables to model performance and spatial transferability.

Therefore, this study aims to develop a machine-learning-based paddy mapping framework that integrates multispectral satellite imagery and multivariate agroecological data. The proposed approach is expected to improve mapping accuracy while enhancing model robustness across heterogeneous agroecological zones. Furthermore, by incorporating environmentally meaningful variables, this study seeks to improve model transferability to other regions with similar agroecological characteristics, offering an efficient and scalable solution to support data-driven precision agriculture and sustainable land management planning.

## 2. METHODS

### 2.1 Research Location

The study was implemented in Banjar City, which is located in the eastern part of West Java, Indonesia. In general, Geographically, Banjar City is located at 108° 26′ – 108° 40′ East Longitude and 07° 19′ – 07° 26′ South Latitude, with the boundaries of the area surrounded by the Regency of Ciamis, almost all sides, and the eastern sea bordering the Regency of Cilacap, Central Java. The area of Banjar City is 131.97 km², as shown in **Figure 1**.

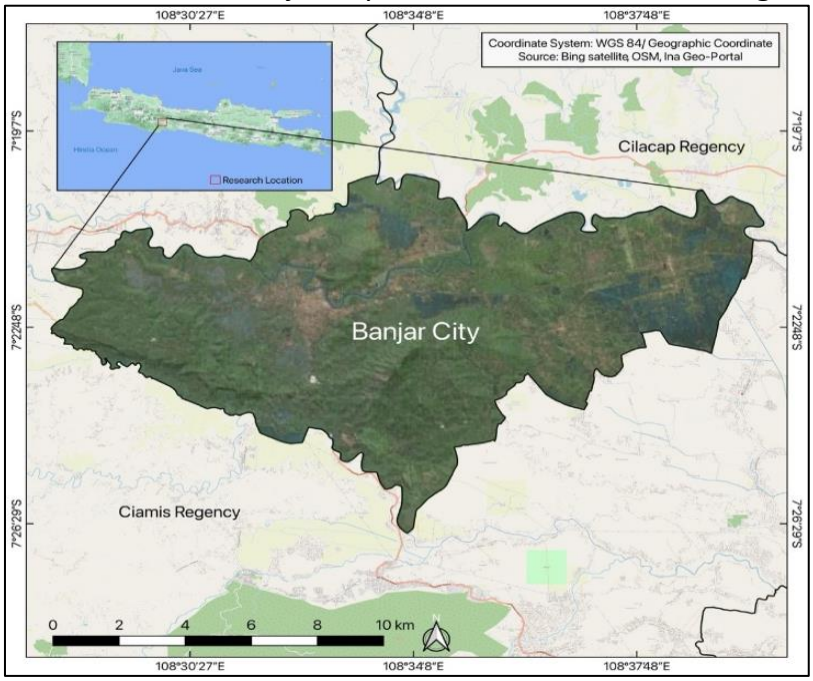



**Figure 1.** Map of Research Locations in Banjar City (Source: Data Processing, 2025)

DOI: https://doi.org/10.17509/gea.v26i1.89942
p-ISSN 1412-0313 e-ISSN 2549-7529

Banjar City was chosen as the location for a study because of its diverse landscape/ relief. Based on the Wargi Jabar webgis data owned by the Department of Public Works and Spatial Planning, it can be known that a large part of Banjar City consists of plains with fluvial landforms, where the middle part of the city is divided by a river, Citanduy. Although the west, north, and south are landforms, they are volcanic and partly structural hills. Variation in the existing landscape is expected to bring out novelty in the study mapping paddy plants based on agroecological data and sensing with machine learning models.

2.2 Research Materials and Tools

The data used is Sentinel-2A with a spatial resolution of 10 m. All data are available from the beginning to the end of 2023, and a filtered image with free < 20% cloud cover is obtained during the paddy planting season from January to December. The data is then processed using Google Earth Engine (https://earthengine.google.com/ ). The reflection data layer at the lower atmosphere (BOA) level L2A was used. Then, Sentinel-2 data was taken, returning to a 10 m resolution with bilinear sampling. Next, the original 60 m resolution band and the edge band red were eliminated. Finally, six bands (Band 2, Band 3, Band 4, Band 8, Band 11, and Band 12) are used in this work.

The other data used is in a limited administration format.shp The Banjar City was the locus of research, and the masking process was carried out on the Sentinel image scene and obtained through the Inageoportal of the *www.tanahair.indonesia.go.id* owned by the Information Agency Geospatial. Validation data modelling plant food using image data with a higher spatial resolution originat*ing from Google Earth.* Validation data prediction production using survey data from the field and interviews with farmers and extension workers in agriculture. Agroecological data and imagery sensing are used far more in the study. This is more evident in Table 1.

**Table 1.** Data Matrix

| No | Data Type | Data source | Year | Resolution |
|---|---|---|---|---|
| 1 | Satellite Imagery Multispectral | Sentinel-2 (COPERNICUS/S2) | 2023 | 10 meters |
| 2 | Rainfall Daily | CHIRPS (UCSB-CHG/CHIRPS/DAILY) | 2023 | ~5.6 km (~0.05°) |
| 3 | Elevation | SRTM (USGS/SRTMGL1_003) | 2000 | 30 meters |
| 4 | Slope Slope | Derivative from SRTM data | 2000 | 30 meters |
| 5 | Direction Slope | Derivative from SRTM data | 2000 | 30 meters |
| 6 | Landform | Derivative from SRTM data | 2000 | 30 meters |
| 7 | Training and Validation Data (Paddy and Non-paddy Labels ) | Digitization/ visual interpretation | 2023 | 10 meters |

2.3 Data Processing and Preparation

Remote sensing and agroecological datasets require careful processing before analysis due to the presence of noise, artefacts, and inconsistencies originating from sensor characteristics, atmospheric conditions, and data acquisition geometry. In this study, multispectral satellite imagery was preprocessed to ensure data quality and consistency, including cloud and cloud-shadow masking, radiometric normalization, and spatial alignment. All images were temporally filtered to match the paddy growing season and resampled to a common spatial resolution to ensure compatibility among datasets. Spectral bands and vegetation indices relevant to crop monitoring were then extracted, while non-agricultural and irrelevant areas were masked to reduce noise and improve classification performance.

DOI: https://doi.org/10.17509/gea.v26i1.89942
p-ISSN 1412-0313 e-ISSN 2549-7529

Agroecological variables, including rainfall, elevation, slope, aspect, and landform information, were processed and standardized to align with the spatial framework of the multispectral imagery. Continuous variables were normalized to minimize scale differences and reduce model bias, while categorical variables were encoded appropriately for machine learning analysis. All datasets were integrated into a unified feature space, allowing each pixel to be represented by both spectral and agroecological attributes. This preprocessing strategy was designed to preserve meaningful information, reduce redundancy, and enhance the ability of machine learning models to capture complex relationships between environmental conditions and paddy distribution.

### 2.4 Mapping Paddy Method

First, a visual interpretation of the paddy plant in Banjar City. Second applied extraction on the features series Sentinel-2 time with transformation *Normalized Difference Vegetation Index (NDVI)* for the point sample plant food. The reconstruction *machine learning* consists of algorithms such as *SVM* and *RF*. Time series *NDVI* is included in the classifier as optimal features, and models are selected by comparing the performance of the results.

Two machine learning classification algorithms, namely SVM and RF, are used in this study. SVM is an algorithm for general linear classification, when make SVM prediction maps data through kernel functions and shares data through limit decision (SMOLA and SCHOLKOPF, 2004). RF is an algorithm consisting of several tree decisions *(decision trees)*, which produce results classification ending with the most (Jin et al., 2017; Month, 2017). *Stacking* is the process of entering results from the base model as a feature into another model. Method: This produces meaningful models that result from layering. First, it uses input from the second layer, and the final layer emits the final result (Menahem, Rokach, and Elovici, 2009). SVM and RF classifier parameters can be seen in Table 2.

**Table 2.** Description of classifier parameters *SVM* and *RF*

| Classifier | Parameter | Information | Value |
|---|---|---|---|
| SVM | C | C is coefficient penalty used For control function loss. | 10 |
| | Gamma | gamma shows coefficient kernel functions. | 0.1 |
| RF | n_estimator | n_estimators show RF capabilities and complexity for study from data. | 300 |
| | min_samples_split | min_samples_split state minimum number of samples required For separate internal nodes. | 2 |
| | min_leaf_sample | min_samples_leaf show tree minimum sample at leaf nodes. | 1 |
| | max_features | max_features means amount must have features under consideration moment find point optimal separation. | sqrt |

Source: (L. Wang, Wang, Zhang, et al., 2022)

### 2.5 Method Model Evaluation

Three metrics, including accuracy, overall F1 score and kappa coefficient, were used in this study to evaluate the performance of the *machine learning* and *deep learning* algorithms (Powers, 2020). All metrics were analyzed using weighted average ( https://scikit-learn.org/ ). When the sample is not balanced, no appropriate method is used to set the same weight for every class, so the weighted average method is used to

DOI: https://doi.org/10.17509/gea.v26i1.89942
p-ISSN 1412-0313 e-ISSN 2549-7529

set different weights for every class in accordance with the size of each class. The number of samples in each class is weighted according to the class. Accuracy overall is the proportion of the total predicted classes that are true, whereas the F1 score is the harmonic mean of precision and recall, which can highlight the ability to identify distribution models of spatial plants. The kappa coefficient shows the balance matrix error and is used for testing consistency.

$$\text{Accuracy overall} = \frac{CP+CN}{CP+FP+FN+CN}$$

$$\text{F1} - \text{score} = 2 \text{ x} \frac{Presisi\ x\ appearance}{Presisi+appearance}$$

$$\text{Kappa coefficient} = \frac{P0-Pe}{1-Pe}$$

Positive and negative show whether or not plants, CP, and FP show prediction true and false positives, and TN and FN indicate true and false predictions, respectively. The matrix confusion is shown in **Table 3**. Precision level shows the proportion of classified data with Correct as a percentage of all data, while the level of withdrawal shows the number of samples in the classified class with Correct as a percentage of the class. p0 is the ratio of diagonal elements of the matrix of confusion to all elements of the matrix, and pe is the ratio of the product amount from the actual and predicted data volume, according to all categories, respectively, and the square of the sample size.

**Table 3.** Matrix error mapped based on predicted and actual classification

| | | **Prediction** | |
|---|---|---|---|
| | | **Positive** | **Negative** |
| Current | Positive | Correct Positive (CP) | False Negative (FN) |
| | Negative | False Positive (FP) | Correct Negative (CN) |

Source: (X. Wang et al., 2022)

Sampling data were collected using a stratified random sampling approach based on landform characteristics to ensure representative coverage of the heterogeneous agroecological conditions within the study area. The research area was stratified into three major landform units fluvial, structural, and volcanic each representing distinct geomorphological and biophysical environments that influence paddy cultivation patterns. Landform delineation was derived from an integrated analysis of a digital elevation model (DEM), slope and curvature derivatives, geological maps, and existing landform classification references. These datasets were combined to identify terrain morphology, drainage patterns, and geological structures, which were then interpreted to delineate fluvial (riverine and alluvial plains), structural (tectonically controlled hills and ridges), and volcanic landforms.

Based on the delineated landform strata, sampling points were allocated proportionally according to the spatial extent of each landform unit. A total of 180 sample points were used for model training and validation, consisting of 80 paddy samples distributed across volcanic (25 points), fluvial (35 points), and structural landforms (20 points), and 100 non-paddy samples representing various non-rice land cover types across the study area (Figure 2). The variation in sample size among landform units reflects their relative areal proportions, with larger landform areas assigned more samples to adequately capture spatial variability. This stratified sampling design ensured balanced representation of landform-driven environmental conditions in both model development and accuracy assessment.

DOI: https://doi.org/10.17509/gea.v26i1.89942
p-ISSN 1412-0313 e-ISSN 2549-7529

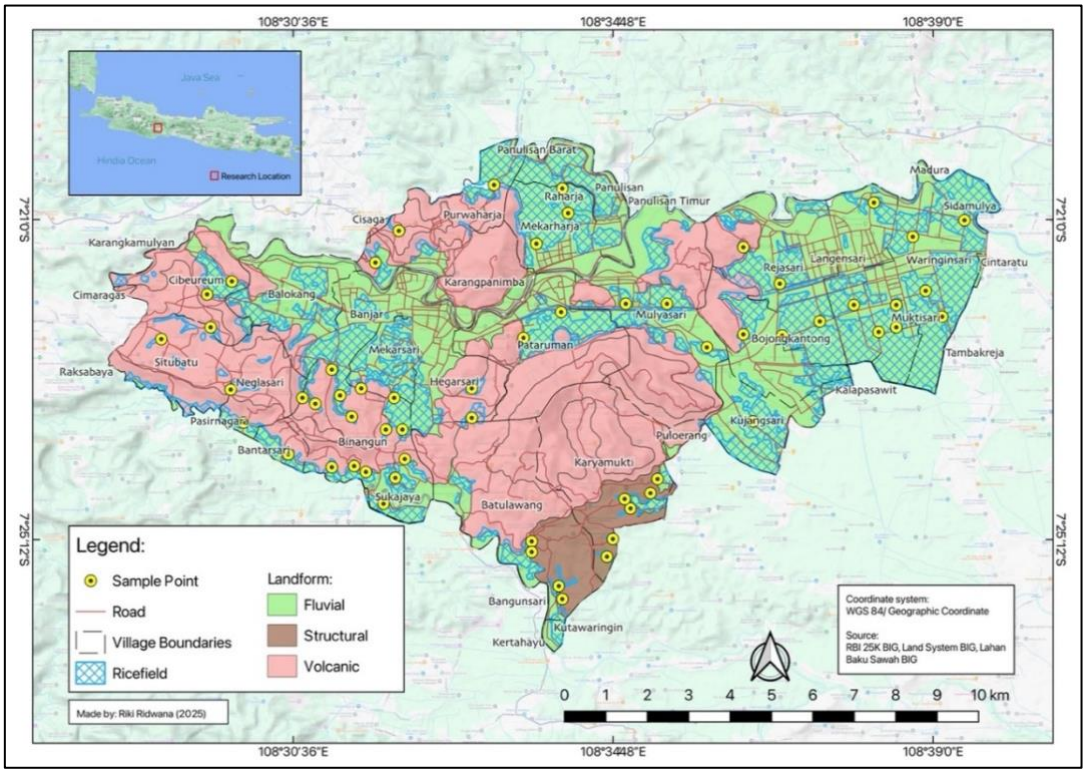



**Figure 2.** Distribution map point Banjar City paddy field sample (Data processing, 2025)

The difference in elevation of the research area was also the basis for determining the sample points, resulting in diverse samples based on height. The elevation lowest is 10 meters above sea level, the average elevation is 36 meters above sea level, and the elevation highest is 145 meters above sea level, with the highest 29.7%, while the average slope is between 3.2% - 3.1%. (Profile elevation point paddy field samples can be seen in **Figure 3**).

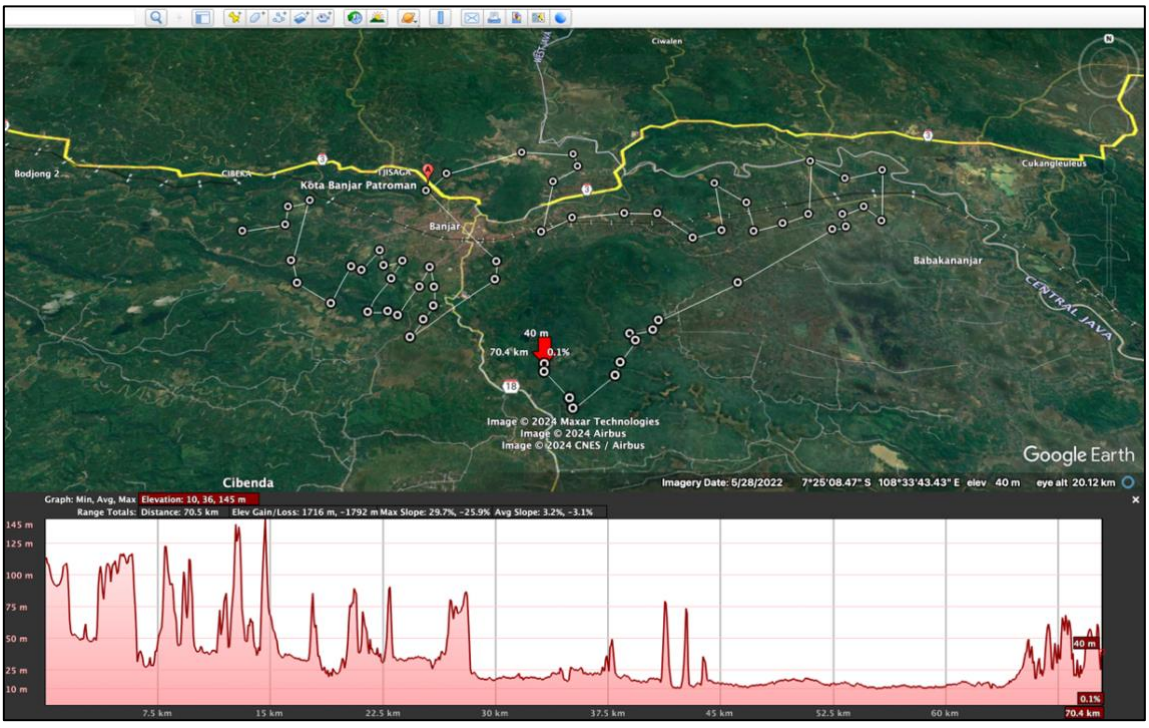



**Figure 3.** Profile elevation point sample ( Data processing, 2024)

DOI: https://doi.org/10.17509/gea.v26i1.89942
p-ISSN 1412-0313 e-ISSN 2549-7529

An overview of the methodological steps used in this study is presented in the research flow diagram shown in Figure 4.

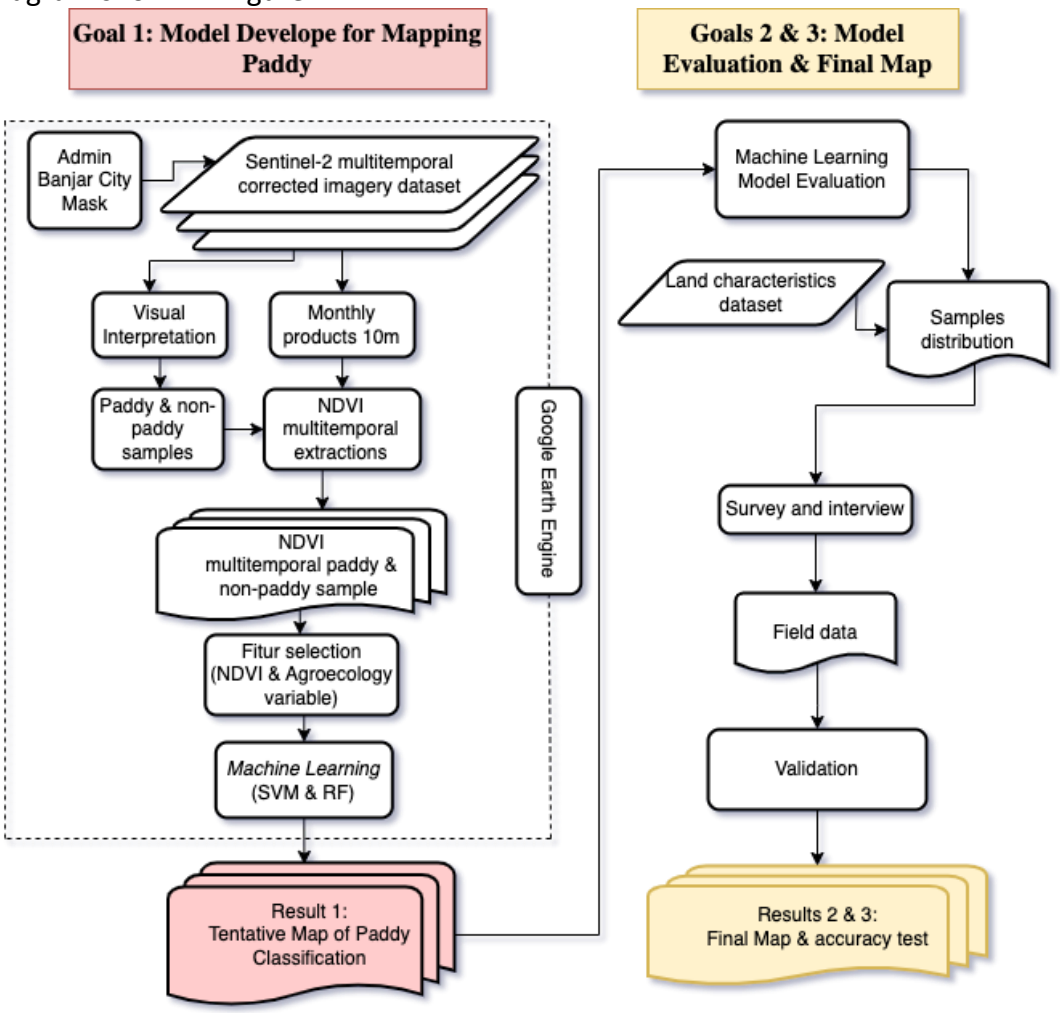



**Figure** 4. Flowchart Study

## 3. RESULTS AND DISCUSSION

### 3.1 Paddy Mapping

#### 3.1.1 Support Vector Machine (SVM) Algorithm

The Support Vector Machine (SVM) algorithm was selected for paddy mapping due to its strong capability to construct an optimal separating hyperplane in high-dimensional feature space, making it well-suited for classifying non-linear and heterogeneous remote sensing data. SVM has been widely applied in agricultural land cover mapping because of its robustness in handling limited and unbalanced training samples, as well as its effectiveness in capturing complex spectral patterns of vegetation (Dang et al., 2021; Kumar et al., 2017; D. Li et al., 2017). In this study, the SVM classifier was used to categorize Sentinel-2 multispectral imagery into two classes: paddy and non-paddy areas.

Figure 5 presents the spatial distribution of paddy fields in Banjar City, West Java, derived from SVM-based classification using Sentinel-2 imagery acquired in 2023. Paddy fields are shown in green, while non-paddy areas are depicted in white. The resulting map provides a comprehensive overview of the spatial extent and distribution of paddy cultivation across the city, offering valuable spatial information to support analyses of agricultural productivity, land management, and regional planning. Similar applications of Sentinel-2 and SVM for paddy mapping have demonstrated reliable spatial representation of rice-growing areas in tropical environments (Nguyen, 2020; Zheng et al., 2015).

DOI: https://doi.org/10.17509/gea.v26i1.89942
p-ISSN 1412-0313 e-ISSN 2549-7529

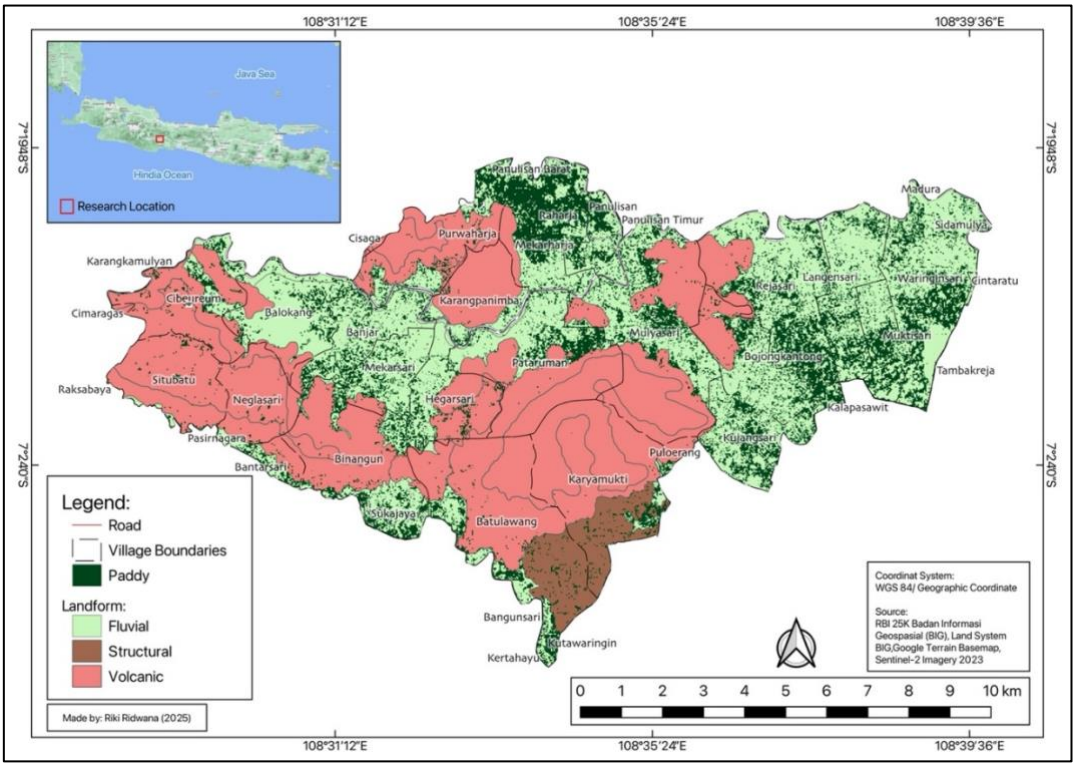



**Figure 5.** Plant Map Paddy 2023 Using SVM Algorithm of Banjar City, West Java ( Data Processing, 2025)

Overall, the spatial pattern of paddy cultivation in Banjar City in 2023 is uneven, with the highest concentration located in the central and eastern parts of the city, particularly in Pataruman District, including the sub-districts of Muktisari and Bojongkantong. These areas correspond to zones of intensive agriculture situated on fluvial landforms, primarily alluvial plains. Such landforms are characterized by relatively flat topography, fertile soil textures resulting from sediment deposition, and reliable water availability from technical and semi-technical irrigation systems. These physical conditions are highly favorable for paddy cultivation, which requires a continuous and sufficient water supply throughout its growth cycle. Previous studies have similarly highlighted the dominance of paddy fields in alluvial and irrigated lowland areas due to their optimal geomorphological and hydrological conditions (Gumma et al., 2022; Murti, 2018).

In contrast, the western and southern parts of Banjar City, including Batulawang and Karyamukti, exhibit a lower density of paddy fields. These areas are predominantly associated with structural and volcanic landforms, which impose greater constraints on paddy cultivation. Structural landforms generally feature undulating to hilly terrain, irregular drainage patterns, and higher susceptibility to erosion, while volcanic landforms often have more permeable soils and limited irrigation infrastructure. These factors reduce water retention capacity and make large-scale paddy cultivation less suitable compared to fluvial plains. This spatial contrast clearly indicates that landform characteristics play a critical role in determining land suitability for paddy agriculture, consistent with findings from previous agroecological and geomorphological studies (Gaznayee, 2019; Lee et al., 2020).

The SVM classifier demonstrated strong capability in identifying paddy cover from Sentinel-2 imagery, particularly in homogeneous and flat agricultural areas. The algorithm effectively captured vegetation spectral signatures, including those associated with active photosynthetic conditions reflected by indices such as the Normalized Difference Vegetation

DOI: https://doi.org/10.17509/gea.v26i1.89942
p-ISSN 1412-0313 e-ISSN 2549-7529

Index (NDVI). The resulting classification shows clear separation between paddy and non-paddy areas in intensively cultivated zones, confirming the suitability of SVM for paddy mapping in complex agricultural landscapes. This finding aligns with earlier studies reporting high classification accuracy of SVM in rice mapping using multispectral data (Belgiu, 2018; Ni et al., 2021).

However, limitations were observed in transitional or boundary areas, particularly where newly ploughed paddy fields, mixed gardens, and non-paddy vegetation coexist. In such areas, spectral similarity between land cover types and fragmented spatial patterns led to misclassification. These challenges are more pronounced in undulating terrains and heterogeneous landscapes, where paddy fields are small, scattered, and spectrally mixed with surrounding vegetation. Similar limitations of SVM in discriminating spectrally similar classes in complex environments have also been reported in previous remote sensing-based agricultural studies (Khanal et al., 2020; Nguyen, 2020; Xiong et al., 2020).

From a spatial planning and land management perspective, the paddy distribution map generated through SVM classification has substantial potential as a decision-support tool. Local governments can use this information to identify priority zones for agricultural intensification, optimize irrigation development in fluvial areas, and design adaptive agricultural strategies for regions with limited geomorphological suitability. Furthermore, the paddy map can serve as a baseline dataset for monitoring agricultural land dynamics in rapidly developing urban and peri-urban areas, supporting sustainable land use planning and food security policies.

### 3.1.2 Random Forest (RF) Algorithm

The Random Forest (RF) algorithm was selected for paddy mapping due to its strong capability to handle high-dimensional datasets and its robustness against overfitting through ensemble learning based on random sampling and feature selection. RF has been widely adopted in agricultural remote sensing because it can effectively model complex, non-linear relationships between multispectral features and land cover classes, particularly in heterogeneous landscapes (Chen et al., 2021; R. Li, 2021).

Figure 6 illustrates the spatial distribution of paddy fields in Banjar City, West Java, generated from the RF-based classification of Sentinel-2 multispectral imagery acquired in 2023. In this map, paddy fields are represented in green, while non-paddy areas are shown in white. Sentinel-2 imagery provides rich multispectral information, including visible, near-infrared, red-edge, and shortwave infrared bands, which are highly sensitive to vegetation structure, moisture conditions, and crop phenology. These spectral characteristics enable effective discrimination between paddy and non-paddy land cover types in tropical agricultural environments (HU et al., 2017; WANG et al., 2012; ZHANG et al., 2019).

The RF classification results indicate that paddy fields are widely distributed across Banjar City, with the highest concentrations occurring in the central and eastern parts of the city, particularly in Pataruman District. These areas are predominantly associated with fluvial landforms, specifically alluvial plains formed through river sedimentation processes. Such landforms are characterized by relatively flat topography, fine soil texture, and abundant surface water availability, making them highly suitable for irrigated paddy cultivation. Similar spatial associations between paddy distribution and fluvial landforms have been reported in recent studies, emphasizing the importance of geomorphological and hydrological conditions in rice-growing regions (Opitz et al., 2023; Sisheber, 2022; H. Zhang et al., 2021).

In contrast, the western and southern parts of Banjar City, including Karangpanimba, Batulawang, and Karyamukti, are dominated by non-paddy land cover. These areas are

DOI: https://doi.org/10.17509/gea.v26i1.89942
p-ISSN 1412-0313 e-ISSN 2549-7529

primarily associated with structural and volcanic landforms. Structural landforms typically exhibit undulating to hilly terrain with uneven natural drainage, while volcanic landforms are characterized by steeper slopes and more porous soils. Such conditions limit water retention and irrigation efficiency, making them less suitable for extensive paddy cultivation. As a result, paddy fields in these areas appear sporadic and fragmented. This pattern is consistent with recent agroecological studies highlighting terrain slope, soil permeability, and irrigation accessibility as key limiting factors for paddy expansion (Lee et al., 2020; Talaviya et al., 2020).

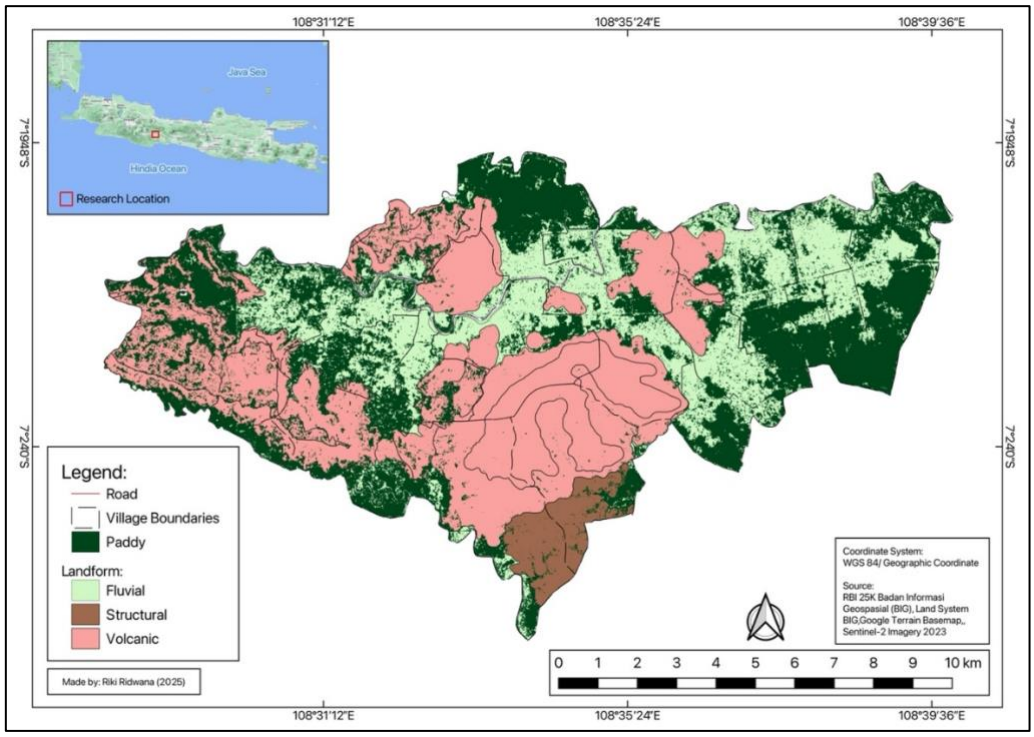



**Figure 6.** Plant Map Paddy Use RF Algorithm of Banjar City, West Java (Data processing, 2025)

The Random Forest algorithm demonstrated strong performance in classifying paddy fields in areas with high spectral and environmental heterogeneity. By aggregating the results of multiple decision trees, RF effectively captured variations in spectral reflectance associated with different paddy growth stages and environmental conditions. Vegetation features derived from Sentinel-2 imagery, such as the Normalized Difference Vegetation Index (NDVI), red-edge bands, and shortwave infrared (SWIR) bands, played a crucial role in distinguishing paddy from other vegetation types. Recent studies have similarly reported that RF performs well in tropical regions where frequent cloud cover and mixed cropping systems pose challenges for crop classification (Todoroff and Kemp, 2016; H. Zhang et al., 2022).

Compared to Support Vector Machine (SVM), RF showed greater classification consistency in areas with mixed vegetation, such as mosaics of paddy fields, gardens, and fallow land. Nevertheless, classification challenges remain in transitional zones, particularly along paddy field boundaries and in areas dominated by grassland or secondary vegetation with similar spectral characteristics. Minor misclassifications in these zones have also been noted in recent RF-based rice mapping studies and are commonly attributed to spectral overlap and spatial fragmentation (Choudhary et al., 2022; Yang and Li, 2022).

From a computational perspective, RF requires longer processing time than SVM due to its ensemble learning structure. However, the resulting paddy distribution map has high

DOI: https://doi.org/10.17509/gea.v26i1.89942
p-ISSN 1412-0313 e-ISSN 2549-7529

strategic value for land use planning and food security management at the local scale. The spatial information generated can support government agencies in identifying priority areas for agricultural intensification, planning irrigation network development, protecting productive paddy land from urban expansion, and directing less suitable areas toward alternative commodities or land and water conservation strategies. Similar policy-relevant applications of RF-based crop maps have been highlighted in recent regional-scale agricultural studies (Belgiu, 2016; Dong and Xiao, 2016; Noi, 2018).

3.2 Machine Learning Model Evaluation and Comparison

The performance of the Support Vector Machine (SVM) and Random Forest (RF) classifiers was evaluated using independent validation datasets and summarized through confusion matrices (**Tables 4**). Both models were assessed using standard accuracy metrics, including Overall Accuracy (OA), Precision, Recall (Sensitivity), F1-score, and the Kappa coefficient, to provide a comprehensive comparison of classification performance in mapping paddy and non-paddy areas.

**Table 4**. Comparison of classification performance between SVM and RF

| Metric | SVM | RF |
|---|---|---|
| Correct Positive (CP) | 38 | 38 |
| Correct Negative (CN) | 45 | 46 |
| False Positive (FP) | 5 | 4 |
| False Negative (FN) | 2 | 2 |
| Overall Accuracy (%) | 92 | 93 |
| Precision (%) | 88 | 90 |
| Recall / Sensitivity (%) | 95 | 95 |
| F1-score (%) | 91 | 92 |
| Kappa Coefficient | 0.84 | 0.86 |

For the SVM model, the confusion matrix results indicate that 45 non-paddy samples were correctly classified as non-paddy (Correct Negative, CN), while 38 paddy samples were correctly identified as paddy (Correct Positive, CP). Misclassifications consisted of 5 non-paddy samples incorrectly classified as paddy (False Positive, FP) and 2 paddy samples misclassified as non-paddy (False Negative, FN). Based on these results, the SVM model achieved an Overall Accuracy of **92%**, a Precision of **88%**, a Recall of **95%**, an F1-score of **91%**, and a Kappa coefficient of **0.84**. These values indicate strong overall performance, particularly in detecting paddy areas, as reflected by the high recall value.

The RF model showed slightly improved classification performance. The confusion matrix indicates that 46 non-paddy samples were correctly classified (CN), and 38 paddy samples were correctly identified (CP). The number of False Positives and False Negatives was reduced to 4 and 2, respectively. Consequently, the RF classifier achieved an Overall Accuracy of **93%**, a Precision of **90%**, a Recall of **95%**, an F1-score of **92%**, and a Kappa coefficient of **0.86**. The higher precision and Kappa values suggest that RF yielded more consistent classification

DOI: https://doi.org/10.17509/gea.v26i1.89942
p-ISSN 1412-0313 e-ISSN 2549-7529

results, particularly in reducing commission errors related to non-paddy areas being misclassified as paddy.

A direct comparison of the two models highlights that both SVM and RF performed well in mapping paddy fields using Sentinel-2 multispectral imagery. However, RF consistently outperformed SVM across most evaluation metrics, particularly in Overall Accuracy, Precision, F1-score, and Kappa coefficient. The identical recall values (95%) indicate that both models were equally effective in capturing actual paddy areas, which is critical for accurate estimation of paddy extent. The superior performance of RF can be attributed to its ensemble learning mechanism, which aggregates multiple decision trees and is more robust to spectral heterogeneity and mixed land cover conditions. Similar findings have been reported in recent rice-mapping studies, where RF demonstrated higher stability and generalization ability compared to SVM in complex tropical agricultural landscapes (Nguyen et al., 2020; Loebel et al., 2022; Li et al., 2023).

Despite the strong performance of both models, minor misclassifications were observed, particularly in transitional zones where paddy fields coexist with other vegetation types or where spectral characteristics overlap. These limitations are commonly reported in machine learning–based crop mapping and highlight the challenges of distinguishing spectrally similar land cover classes using single-date imagery (Li et al., 2023). Incorporating multi-temporal observations or additional agroecological variables may further improve classification accuracy and model robustness.

Overall, the comparative evaluation demonstrates that both SVM and RF are reliable classifiers for paddy mapping at the municipal scale. However, RF shows a slight advantage in terms of classification consistency and agreement beyond random chance, making it more suitable for operational paddy mapping and decision-support applications. The validated classification results provide a robust spatial basis for agricultural planning, irrigation management, and food security assessment in Banjar City.

## 4. CONCLUSIONS

This study demonstrates that integrating multispectral Sentinel-2 imagery with agroecological variables significantly improves the spatial accuracy of paddy mapping. The incorporation of environmental context, including landforms and related biophysical factors, enhances machine learning models' ability to capture the complex spatial and spectral characteristics of paddy fields in tropical agricultural landscapes. Both Support Vector Machine (SVM) and Random Forest (RF) algorithms achieved high classification performance, with overall accuracy exceeding 90%, confirming their effectiveness for paddy identification at the municipal scale.

Comparative evaluation shows that Random Forest slightly outperformed Support Vector Machine across overall accuracy, precision, F1-score, and Kappa coefficient, while both models achieved equally high recall in detecting paddy areas. These findings highlight the robustness of ensemble-based approaches in handling spectral heterogeneity and mixed land cover conditions commonly found in tropical regions. More importantly, the results emphasize the critical role of integrating agroecological information into machine learning frameworks, rather than relying solely on spectral features.

The proposed spatial–contextual paddy mapping framework provides a scalable and transferable approach that can be applied to other regions with similar agroecological characteristics. This approach has practical implications for supporting data-driven agricultural planning, irrigation management, and food security assessment. Future work

DOI: https://doi.org/10.17509/gea.v26i1.89942
p-ISSN 1412-0313 e-ISSN 2549-7529

should explore the use of multi-temporal imagery and additional environmental variables further to enhance model robustness and applicability across diverse agroecological zones.

## 5. RECOMMENDATIONS

To support evidence-based decision-making in the agricultural sector, it is recommended that national and regional agricultural and food planning agencies adopt integrative approaches combining remote sensing and machine learning. The results of this study demonstrate that such approaches can provide timely, accurate, and spatially explicit information on paddy distribution, which is essential for effective agricultural management and policy formulation.

The development of cloud-based precision agriculture monitoring systems, such as Google Earth Engine, should be further expanded by explicitly incorporating agroecological variability and local environmental conditions. Accounting for spatial heterogeneity in landform, hydrology, and climate can enhance model reliability and applicability across diverse agricultural regions. In addition, future research should evaluate the performance of the proposed mapping framework under extreme environmental conditions, such as prolonged droughts or flood events, to improve its robustness and support climate change adaptation strategies in agricultural planning.

## 6. REFERENCES

Arrafi, M., Somantri, L., and Ridwana, R. (2022). Pemetaan Tingkat Keparahan Kebakaran Hutan dan Lahan Menggunakan Algoritma Normalized Burn Ratio (NBR) Pada Citra Landsat 8 di Kabupaten Muaro Jambi. *Jurnal Geosains Dan Remote Sensing*, *3*(1), 10–19. https://doi.org/10.23960/jgrs.2022.v3i1.68

Belgiu, M. (2016). Random forest in remote sensing: A review of applications and future directions. In *ISPRS Journal of Photogrammetry and Remote Sensing* (Vol. 114, pp. 24–31). https://doi.org/10.1016/j.isprsjprs.2016.01.011

Belgiu, M. (2018). Sentinel-2 cropland mapping using pixel-based and object-based time-weighted dynamic time warping analysis. *Remote Sensing of Environment*, *204*, 509–523. https://doi.org/10.1016/j.rse.2017.10.005

Chen, Y., Hou, J., Huang, C., Zhang, Y., and Li, X. (2021). Mapping maize area in heterogeneous agricultural landscape with multi-temporal sentinel-1 and sentinel-2 images based on random forest. *Remote Sensing*. https://www.mdpi.com/2072-4292/13/15/2988

Choudhary, K., Shi, W., Dong, Y., and Paringer, R. (2022). Random Forest for rice yield mapping and prediction using Sentinel-2 data with Google Earth Engine. *Advances in Space Research*, *70*(8), 2443–2457. https://doi.org/https://doi.org/10.1016/j.asr.2022.06.073

Dang, C., Liu, Y., Yue, H., Qian, J. X., and Zhu, R. (2021). Autumn Crop Yield Prediction using Data-Driven Approaches:- Support Vector Machines, Random Forest, and Deep Neural Network Methods. *Canadian Journal of Remote Sensing*, *47*(2), 162–181. https://doi.org/10.1080/07038992.2020.1833186

Dharma, F., Aulia, A., Shubhan, F., and Ridwana, R. (2022). Pemanfaatan Citra Sentinel - 2 Dengan Metode NDVI Untuk Perubahan KerapatanVegetasi Mangrove Di Kabupaten Indramayu. *J Pendidikan Geografi Undiksha*, *10*(2), 155–165.

Dong, J., and Xiao, X. (2016). Evolution of regional to global paddy rice mapping methods: A review. In *ISPRS Journal of Photogrammetry and Remote Sensing* (Vol. 119, pp. 214–227). Elsevier B.V. https://doi.org/10.1016/j.isprsjprs.2016.05.010

Gaznayee, H. A. A. (2019). Analysis of agricultural drought, rainfall, and crop yield relationships in erbil province, the kurdistan region of iraq based on landsat time-series

msavi2. *Journal of Advanced Research in Dynamical and Control Systems*, *11*(12), 536–545. https://doi.org/10.5373/JARDCS/V11SP12/20193249

Gumma, M. K., Thenkabail, P. S., Panjala, P., Teluguntla, P., Yamano, T., and Mohammed, I. (2022). Multiple agricultural cropland products of South Asia developed using Landsat-8 30 m and MODIS 250 m data using machine learning on the Google Earth Engine (GEE) cloud and spectral matching techniques (SMTs) in support of food and water security. *GIScience and Remote Sensing*, *59*(1), 1048–1077. https://doi.org/10.1080/15481603.2022.2088651

HU, Q., WU, W., SONG, Q., LU, M., CHEN, D., YU, Q., and TANG, H. (2017). How do temporal and spectral features matter in crop classification in Heilongjiang Province, China? *Journal of Integrative Agriculture*, *16*(2), 324–336. https://doi.org/https://doi.org/10.1016/S2095-3119(15)61321-1

Jin, S., Yang, L., Zhu, Z., and Homer, C. (2017). A land cover change detection and classification protocol for updating Alaska NLCD 2001 to 2011. *Remote Sensing of Environment*, *195*, 44–55. https://doi.org/10.1016/j.rse.2017.04.021

Kadir, P. :, Jakarta, R., and Juli, I. (2019). *Memperbaiki Data Pangan Indonesia Lewat Metode Kerangka Sampel Area*.

Khanal, S., Kushal, K. C., Fulton, J. P., Shearer, S., and Ozkan, E. (2020). Remote sensing in agriculture—accomplishments, limitations, and opportunities. In *Remote Sensing* (Vol. 12, Issue 22, pp. 1–29). MDPI AG. https://doi.org/10.3390/rs12223783

Klerkx, L., Jakku, E., and Labarthe, P. (2019). A review of social science on digital agriculture, smart farming and agriculture 4.0: New contributions and a future research agenda. *NJAS - Wageningen Journal of Life Sciences*, *90–91*(November), 100315. https://doi.org/10.1016/j.njas.2019.100315

Kumar, S., Mishra, S., Khanna, P., and Pragya. (2017). Precision Sugarcane Monitoring Using SVM Classifier. *Procedia Computer Science*, *122*, 881–887. https://doi.org/10.1016/j.procs.2017.11.450

Lee, R. Y., Chang, K. C., Ou, D. Y., and Hsu, C. H. (2020). Evaluation of crop mapping on fragmented and complex slope farmlands through random forest and object-oriented analysis using unmanned aerial vehicles. *Geocarto International*, *35*(12), 1293–1310. https://doi.org/10.1080/10106049.2018.1559886

Li, D., Yang, F., and Wang, X. (2017). Study on Ensemble Crop Information Extraction of Remote Sensing Images Based on SVM and BPNN. *Journal of the Indian Society of Remote Sensing*, *45*(2), 229–237. https://doi.org/10.1007/s12524-016-0597-y

Li, R. (2021). Phenology-based classification of crop species and rotation types using fused MODIS and Landsat data: The comparison of a random-forest-based model and a decision-rule-based model. *Soil and Tillage Research*, *206*. https://doi.org/10.1016/j.still.2020.104838

Loebel, E., Scheinert, M., Horwath, M., Heidler, K., Christmann, J., Phan, L. D., ... & Zhu, X. X. (2022). Extracting glacier calving fronts by deep learning: The benefit of multispectral, topographic, and textural input features. *IEEE Transactions on Geoscience and Remote Sensing*, *60*, 1-12.

Menahem, E., Rokach, L., and Elovici, Y. (2009). Troika - An improved stacking schema for classification tasks. *Information Sciences*, *179*(24), 4097–4122. https://doi.org/10.1016/j.ins.2009.08.025

Month, T. (2017). *Nmeth.4370*. *14*(8), 757–759.

Murti, S. (2017). Mapping agroecosystem zone using remote sensing for food security analysis in Bantul district Daerah Istimewa Yogyakarta. In *Proceedings of SPIE - The International Society for Optical Engineering* (Vol. 10421). https://doi.org/10.1117/12.2278011

Murti, S. (2018). Remote sensing and GIS model for food security mapping in Gunungkidul Regency Daerah Istimewa Yogyakarta. In *Proceedings of SPIE - The International Society for Optical Engineering* (Vol. 10777). https://doi.org/10.1117/12.2324029

Nguyen, M. D. (2020). Harmonization of landsat and sentinel 2 for crop monitoring in drought prone areas: Case studies of Ninh Thuan (Vietnam) and Bekaa (Lebanon). *Remote Sensing*, *12*(2). https://doi.org/10.3390/rs12020281

Ni, R., Tian, J., Li, X., Yin, D., Li, J., Gong, H., Zhang, J., Zhu, L., and Wu, D. (2021). An enhanced pixel-based phenological feature for accurate paddy rice mapping with Sentinel-2 imagery in Google Earth Engine. *ISPRS Journal of Photogrammetry and Remote Sensing*, *178*, 282–296. https://doi.org/https://doi.org/10.1016/j.isprsjprs.2021.06.018

Noi, P. T. (2018). Comparison of random forest, k-nearest neighbor, and support vector machine classifiers for land cover classification using sentinel-2 imagery. *Sensors (Switzerland)*, *18*(1). https://doi.org/10.3390/s18010018

Opitz, R., De Smedt, P., Mayoral-Herrera, V., Campana, S., Vieri, M., Baldwin, E., Perna, C., Sarri, D., and Verhegge, J. (2023). Practicing Critical Zone Observation in Agricultural Landscapes: Communities, Technology, Environment and Archaeology. *Land*, *12*(1). https://doi.org/10.3390/land12010179

Powers, D. M. W. (2020). *Evaluation: from precision, recall and F-measure to ROC, informedness, markedness and correlation*. 37–63.

Prasetya, R., and Danoedoro, P. (2019). Paddy and non-paddy crops mapping using multi-temporal data of Sentinel-1A in part of Bantul Regency. *Sixth International Symposium on …*. https://doi.org/10.1117/12.2540635.short

Putra, M. A. B., Nuarsa, I. W., and Adnyana, I. W. S. (2018). Estimasi Produksi Padi dengan Analisis Citra Satelit Landsat 8 di Kabupaten Klungkung Provinsi Bali. *Ecotrophic*, *12*(1), 93-103.

Ridwana, R., Al Kautsar, A., Saleh, F., Himayah, S., Arrasyid, R., and Pamungkas, T. D. (2022). Spatiotemporal monitoring of rice crops in the covid-19 pandemic period for local food security using sentinel 2b imagery case ctudy: tasikmalaya city. *IOP Conference Series: Earth and Environmental Science*, *1089*(1). https://doi.org/10.1088/1755-1315/1089/1/012039

Ridwana, R., Kamal, M., Arjasakusuma, S., and Rabbi, M. F. A. (2024). Evaluation of Machine Learning Models for Mapping Food Crops using Sentinel-2A Imagery in West Java, Indonesia. *E3S Web of Conferences*, *600*. https://doi.org/10.1051/e3sconf/202460003007

Ridwana, R., Kamal, M., Arjasakusuma, S., Sugandi, D., and Sakti, A. D. (2025). Bibliometric Computation Mapping Analysis of Publication Machine and Deep Learning for Food Crops Mapping using VOSviewer. *Journal of Advanced Research in Applied Sciences and Engineering Technology*, *50*(2), 42–59. https://doi.org/10.37934/araset.50.2.4259

Singh, G., Kalra, N., Yadav, N., Sharma, A., and Saini, M. (2022). Smart Agriculture: a Review. *Siberian Journal of Life Sciences and Agriculture*, *14*(6), 423–454. https://doi.org/10.12731/2658-6649-2022-14-6-423-454

Sisheber, B. (2022). Tracking crop phenology in a highly dynamic landscape with knowledge-based Landsat–MODIS data fusion. *International Journal of Applied Earth Observation and Geoinformation*, *106*. https://doi.org/10.1016/j.jag.2021.102670

SMOLA, A. J., and SCHOLKOPF, B. (2004). A tutorial on support vector regression. *Statistics and Computing*, *14*, 199–222. http://citeseerx.ist.psu.edu/viewdoc/download;jsessionid=1CAD92EF8CCE726A305D8A41F873EEFC?doi=10.1.1.114.4288andrep=rep1andtype=pdf%0Ahttp://download.springer.com/static/pdf/493/art%3A10.1023%2FB%3ASTCO.0000035301.49549.88.pdf?auth66=1408162706_8a28764ed0fae9

Song, X. P., Huang, W., Hansen, M. C., and Potapov, P. (2021). An evaluation of Landsat, Sentinel-2, Sentinel-1 and MODIS data for crop type mapping. In *Science of Remote Sensing*. Elsevier. https://www.sciencedirect.com/science/article/pii/S2666017221000055

Stevens, F. (2015). Disaggregating census data for population mapping using Random forests with remotely-sensed and ancillary data. *PLoS ONE*, *10*(2). https://doi.org/10.1371/journal.pone.0107042

Talaviya, T., Shah, D., Patel, N., Yagnik, H., and Shah, M. (2020). Implementation of artificial intelligence in agriculture for optimisation of irrigation and application of pesticides and herbicides. *Artificial Intelligence in Agriculture*, *4*, 58–73. https://doi.org/https://doi.org/10.1016/j.aiia.2020.04.002

Teluguntla, P., Thenkabail, P., Oliphant, A., Xiong, J., Gumma, M. K., Congalton, R. G., Yadav, K., and Huete, A. (2018). A 30-m landsat-derived cropland extent product of Australia and China using random forest machine learning algorithm on Google Earth Engine cloud computing platform. *ISPRS Journal of Photogrammetry and Remote Sensing*, *144*(February), 325–340. https://doi.org/10.1016/j.isprsjprs.2018.07.017

Todoroff, P., and Kemp, J. (2016). *5 - Contribution of Remote Sensing to Crop Monitoring in Tropical Zones* (N. Baghdadi and M. B. T.-L. S. R. S. in A. and F. Zribi, Eds.; pp. 179–220). Elsevier. https://doi.org/https://doi.org/10.1016/B978-1-78548-103-1.50005-4

Tun, S. B. M. (2022). Crop Monitoring of Paddy Field Using Landsat 8 OLI. *International Journal of Geoinformatics*, *18*(4), 35–43. https://doi.org/10.52939/ijg.v18i4.2255

Veloso, A. (2017). Understanding the temporal behavior of crops using Sentinel-1 and Sentinel-2-like data for agricultural applications. *Remote Sensing of Environment*, *199*, 415–426. https://doi.org/10.1016/j.rse.2017.07.015

Wang, L., Wang, J., Liu, Z., Zhu, J., and Qin, F. (2022). Evaluation of a deep-learning model for multispectral remote sensing of land use and crop classification. *The Crop Journal*, *10*(5), 1435–1451. https://doi.org/https://doi.org/10.1016/j.cj.2022.01.009

Wang, L., Wang, J., Zhang, X., Wang, L., and Qin, F. (2022). Deep segmentation and classification of complex crops using multi-feature satellite imagery. *Computers and Electronics in Agriculture*, *200*, 107249. https://doi.org/https://doi.org/10.1016/j.compag.2022.107249

WANG, W., YAO, X., TIAN, Y. chao, LIU, X. jun, NI, J., CAO, W. xing, and ZHU, Y. (2012). Common Spectral Bands and Optimum Vegetation Indices for Monitoring Leaf Nitrogen Accumulation in Rice and Wheat. *Journal of Integrative Agriculture*, *11*(12), 2001–2012. https://doi.org/10.1016/S2095-3119(12)60457-2

Wang, X., Zhang, J., Xun, L., Wang, J., Wu, Z., Henchiri, M., Zhang, S., Zhang, S., Bai, Y., Yang, S., Li, S., and Yu, X. (2022). Evaluating the Effectiveness of Machine Learning and Deep Learning Models Combined Time-Series Satellite Data for Multiple Crop Types Classification over a Large-Scale Region. *Remote Sensing*, *14*(10). https://doi.org/10.3390/rs14102341

DOI: https://doi.org/10.17509/gea.v26i1.89942
p-ISSN 1412-0313 e-ISSN 2549-7529

Xiong, J., Liu, Z., Chen, S., Liu, B., Zheng, Z., Zhong, Z., Yang, Z., and Peng, H. (2020). Visual detection of green mangoes by an unmanned aerial vehicle in orchards based on a deep learning method. *Biosystems Engineering*, *194*, 261–272. https://doi.org/10.1016/j.biosystemseng.2020.04.006

Yang, Y., Huang, Q., Wu, Z., Wu, T., Luo, J., Dong, W., Sun, Y., Zhang, X., and Zhang, D. (2022). Mapping crop leaf area index at the parcel level via inverting a radiative transfer model under spatiotemporal constraints: A case study on sugarcane. *Computers and Electronics in Agriculture*, *198*, 107003. https://doi.org/https://doi.org/10.1016/j.compag.2022.107003

Yang, Y., and Li, X. (2022). Automatic Correction of Parameters of Rice Phenology Prediction Model Based on Random Forest Algorithm. *Procedia Computer Science*, *208*, 435–441. https://doi.org/https://doi.org/10.1016/j.procs.2022.10.061

Zhang, H., Liu, W., and Zhang, L. (2022). Seamless and automated rapeseed mapping for large cloudy regions using time-series optical satellite imagery. *ISPRS Journal of Photogrammetry and Remote Sensing*, *184*, 45–62. https://doi.org/https://doi.org/10.1016/j.isprsjprs.2021.12.001

Zhang, H., Wang, Y., Shang, J., Liu, M., and Li, Q. (2021). Investigating the impact of classification features and classifiers on crop mapping performance in heterogeneous agricultural landscapes. *International Journal of Applied Earth Observation and Geoinformation*, *102*, 102388. https://doi.org/https://doi.org/10.1016/j.jag.2021.102388

Zhang, W., Liu, H., Wu, W., Zhan, L., and Wei, J. (2020). Mapping rice paddy based on machine learning with sentinel-2 multi-temporal data: Model comparison and transferability. *Remote Sensing*, *12*(10). https://doi.org/10.3390/rs12101620

ZHANG, X., LIU, J., Qin, Z., and QIN, F. (2019). Winter wheat identification by integrating spectral and temporal information derived from multi-resolution remote sensing data. *Journal of Integrative Agriculture*, *18*(11), 2628–2643. https://doi.org/https://doi.org/10.1016/S2095-3119(19)62615-8

Zhao, R., Li, Y., and Ma, M. (2021). Mapping paddy rice with satellite remote sensing: A review. In *Sustainability (Switzerland)* (Vol. 13, Issue 2, pp. 1–20). MDPI AG. https://doi.org/10.3390/su13020503

Zheng, B., Myint, S. W., Thenkabail, P. S., and Aggarwal, R. M. (2015). A support vector machine to identify irrigated crop types using time-series Landsat NDVI data. *International Journal of Applied Earth Observation and Geoinformation*, *34*(1), 103–112. https://doi.org/10.1016/j.jag.2014.07.002

DOI: https://doi.org/10.17509/gea.v26i1.89942
p-ISSN 1412-0313 e-ISSN 2549-7529